

Estimate of the hadronic production of the doubly charmed baryon Ξ_{cc} in the general-mass variable-flavor-number scheme

Chao-Hsi Chang,^{1,2,*} Cong-Feng Qiao,^{3,†} Jian-Xiong Wang,^{4,‡} and Xing-Gang Wu^{2,§}

¹CCAST (World Laboratory), P.O.Box 8730, Beijing 100080, People's Republic of China

²Institute of Theoretical Physics, Chinese Academy of Sciences, P.O.Box 2735, Beijing 100080, People's Republic of China

³Department of Physics, Graduate School of the Chinese Academy of Sciences, Beijing 100049, People's Republic of China

⁴Institute of High Energy Physics, P.O.Box 918(4), Beijing 100049, People's Republic of China

(Received 5 January 2006; revised manuscript received 6 April 2006; published 24 May 2006)

To try to understand the experimental observation of SELEX Collaboration and to check the existent results in literature, we have done a theoretical investigation on hadronic production of the doubly charmed baryon Ξ_{cc} (Ξ_{cc}^{++} or Ξ_{cc}^+) under the general-mass variable-flavor-number (GM-VFN) scheme. A similar study of the production at LHC and TEVATRON is also performed. The production here is realized via production of a binding diquark either $(cc)[^3S_1]_{\bar{3}}$ (in configuration S -wave and in color $\bar{3}$) or $(cc)[^1S_0]_6$ (in configuration S -wave and in color 6) instead of only the diquark $(cc)[^3S_1]_{\bar{3}}$ is considered. Numerical results show that the production via each configuration of the diquark is comparable at LHC and TEVATRON under the condition that the NRQCD matrix elements relevant to the diquark production are assumed approximately to be equal to each other; and the contributions from collision of a so-called “extrinsic” charm and a gluon inside the colliding hadrons are comparable with, or even greater than, those from the so-called gluon-gluon fusion, especially, in the region of small transverse-momentum p_t . We also note that due to the contributions from the “extrinsic” charm, the theoretical prediction on the production of the baryon Ξ_{cc} is raised by one order in comparison with the existent predictions almost.

DOI: [10.1103/PhysRevD.73.094022](https://doi.org/10.1103/PhysRevD.73.094022)

PACS numbers: 14.20.Lq, 13.85.Ni, 12.38.Bx

I. INTRODUCTION

The heavy hadron Ξ_{cc}^+ has been observed by SELEX Collaboration probably [1,2], nevertheless, there are some comments [3] that the measured lifetime is much shorter and the production rate is much larger than most of the theoretical predictions. The theoretical estimates predicted that, of the total sample at the fixed target experiment SELLEX, about 10^{-5} of Λ_c^+ events would be produced via Ξ_{cc}^+ decay accordingly [4–8], whereas, the SELEX collaboration found that almost 20% of Λ_c^+ events in their sample were produced via Ξ_{cc}^+ decay.

In literature, most of the perturbative QCD (pQCD) calculations and predictions for Ξ_{cc}^+ hadroproduction are based on the ‘gluon-gluon fusion mechanism’ i.e. via the subprocess $g + g \rightarrow (cc)[^3S_1]_{\bar{3}} + \bar{c} + \bar{c}$, and only one diquark configuration $(cc)[^3S_1]_{\bar{3}}$ is considered. In fact, the mechanism with the subprocess $g + g \rightarrow (cc)[^1S_0]_6 + \bar{c} + \bar{c}$ (via another diquark configuration $(cc)[^1S_0]_6$) may also contribute to the production as pointed out in [9]. It is because that Ξ_{cc}^+ and Ξ_{cc}^{++} may also contain the component $(ccqg)$ (here $q = u, d$) in their Fock space expansion.

According to the reaction time scale, an inclusive production of Ξ_{cc}^+ or Ξ_{cc}^{++} can be divided into three steps: the first step is to produce two c quarks, that generally can be

calculated by pQCD, then the second step is to make these two c quarks into a binding diquark either $(cc)_{\bar{3}}[^3S_1]$ or $(cc)_6[^1S_0]$, that can be described by a matrix element accordingly in nonrelativistic QCD (NRQCD) framework [10], the third step is the diquark hadronizes either into Ξ_{cc}^+ by absorbing a quark d or into Ξ_{cc}^{++} by absorbing a quark u for $(cc)_{\bar{3}}[^3S_1]$, or hadronizes either into Ξ_{cc}^+ by absorbing a quark d and an additional soft gluon or into Ξ_{cc}^{++} by absorbing a quark u and an additional soft gluon for $(cc)_6[^1S_0]$. But so far for the hadronic production of Ξ_{cc} in literature, only the configuration of the binding (cc) -diquark in the $\bar{3}$ color representation and in S -wave 3S_1 is taken into account. Whereas, according to power counting of NRQCD in v_c (the velocity of the heavy c -quarks in the baryon), the matrix elements h_1 and h_3 are at the same order of v_c [9]. Here h_1 depicts the non-perturbative transition from the two charm quarks to the diquark in the configuration $(cc)_6[^1S_0]$ and h_3 depicts that in the configuration $(cc)_{\bar{3}}[^3S_1]$, and their precise definitions are given in Eq. (3). Hence to make an estimation of the hadronic production of Ξ_{cc} , we think that $(cc)_{\bar{3}}[^3S_1]$ and $(cc)_6[^1S_0]$ should be treated on equal footing.

In Ref. [9], the production of Ξ_{cc} at e^+e^- collider is treated carefully and the (cc) -diquark in two configurations $(cc)_{\bar{3}}[^3S_1]$ and $(cc)_6[^1S_0]$ are considered. For the hadronic production, in Ref. [9], it is estimated roughly by comparing it with c -quark jet and both by taking the fragmentation approach. Since the fragmentation approach becomes well only at the high p_t region (e.g. $p_t \gtrsim 25 \sim 30$ GeV [6]) where the fragmentation mechanism is dominant, and the results from the fragmentation

*Electronic address: zhangzx@itp.ac.cn

†Electronic address: qiaocf@gucas.ac.cn

‡Electronic address: jxwang@mail.ihep.ac.cn

§Electronic address: wuxg@itp.ac.cn

¹Throughout the paper, Ξ_{cc} denotes Ξ_{cc}^+ or Ξ_{cc}^{++} , i.e., the isospin-breaking effects are ignorable here.

approach show a strong dependence on the parameter values [9], so in the present work we will take the full pQCD approach to proceed our investigation.

It was noticed that the mechanisms for hadroproduction relevant to charm quark may give sizable contributions to the charmonium production [11], and to the B_c production in small p_t region [12]. Note that the charm ingredients as the PDFs used in Refs. [11,12] are taken from CTEQ6L (for ZM-FNN scheme) and CTEQ6HQ (for massive charm scheme) [13], and they are generated by gluon splitting according to DGLAP evolution. Therefore to be more proper, we should refer the relevant mechanism as ‘‘extrinsic charm’’ mechanism rather than ‘‘intrinsic charm’’ mechanism as sometimes confusedly used in literature. The ‘‘extrinsic’’ charm component in the PDFs is different from the ‘‘intrinsic’’ charm, discussed in Ref. [14], where the ‘‘intrinsic charm’’ has nonperturbative nature and is directly connected to the proton wave function.

Therefore, from the experiences gained from Refs. [11,12] and bearing the difference between SELEX data and the existent theoretical predictions in mind, it is interesting to re-estimate the production of Ξ_{cc}^+ and Ξ_{cc}^{++} precisely, to take into account the two configurations of the diquarks in different color representation $\mathbf{\bar{3}}$ and $\mathbf{6}$, and the ‘‘extrinsic charm mechanisms’’ via the subprocesses of charm creation: $g + c \rightarrow (cc)[^3S_1]_{\mathbf{\bar{3}}} + \bar{c}$, $g + c \rightarrow (cc)[^1S_0]_{\mathbf{6}} + \bar{c}$; via the subprocesses of LO extrinsic charm fusion: $c + c \rightarrow (cc)[^3S_1]_{\mathbf{\bar{3}}}$, $c + c \rightarrow (cc)[^1S_0]_{\mathbf{6}}$ and via the subprocesses of NLO extrinsic charm fusion: $c + c \rightarrow (cc)[^3S_1]_{\mathbf{\bar{3}}} + g$, $c + c \rightarrow (cc)[^1S_0]_{\mathbf{6}} + g$ etc, especially to pay attention to small p_t region of the production.

For a fixed target experiment of SELEX, a comparatively small transverse momentum p_t region of the doubly charmed baryon Ξ_{cc} can be reached, hence, the estimate of the production on the mechanisms mentioned above should be treated more carefully in small p_t region than the existent ones. However we should note that because the available PDFs do not keep the transverse momentum of the partons at all, the LO extrinsic charm fusion mechanisms via the subprocesses $c + c \rightarrow (cc)[^3S_1]_{\mathbf{\bar{3}}}$ and $c + c \rightarrow (cc)[^1S_0]_{\mathbf{6}}$ contribute to the production with zero p_t only. Because of the fact that there still is a small $p_t \sim$

0.2 GeV cut in the SELEX observation, we will not only consider the LO extrinsic charm fusion mechanisms in the paper, we will also consider more mechanisms than those have been considered in the existent theoretical estimates. To cover p_t region as wide as possible, in such a small region $p_t \simeq \mathcal{O}(m_c)$ of the production, the charm mass cannot be ignored, so in the re-estimate we will adopt the general-mass variable-flavor-number (GM-VFN) scheme [15–17]. In the scheme, special attention to the so-called extrinsic charm mechanisms via the subprocesses $g + c \rightarrow (cc)[^3S_1]_{\mathbf{\bar{3}}} + \bar{c}$, $g + c \rightarrow (cc)[^1S_0]_{\mathbf{6}} + \bar{c}$, $c + c \rightarrow (cc)[^3S_1]_{\mathbf{\bar{3}}} + g$ and $c + c \rightarrow (cc)[^1S_0]_{\mathbf{6}} + g$ will be paid.²

In principle, under the GM-VFN scheme to obtain the final result by combining the contributions from various mechanisms, one needs to make some proper subtractions so as to avoid ‘‘double counting’’. In the GM-VFN scheme, the hard-scattering amplitude and the PDFs for the production should be treated in a consistent way. In the paper the up-dated PDFs CTEQ6HQ which are determined by global fitting utilizing massive hard-scattering cross-sections [13] is adopted and matches to the amplitude of the next leading order for the extrinsic charmed mechanisms for the GM-VFN scheme.

The paper is organized as follows. In Sec. II, we shall first give the formulation for the hadronic production of Ξ_{cc} under the GM-VFN scheme, and then present in some more detail the formulae for both the gluon-gluon mechanism and the ‘‘extrinsic’’ charm mechanisms. In Sec. III, we present the results for the subprocesses and make a comparison with those in literature. In Sec. IV, we present the numerical results for the hadronic production of Ξ_{cc} and make some discussion over them. The final section is reserved for a summary. In Appendices some more details on the calculation technologies are presented.

II. FORMULATION UNDER THE GM-VFN SCHEME

According to pQCD factorization theorem, the cross-section for the hadronic production of Ξ_{cc} under the general-mass variable-flavor-number (GM-VFN) scheme up to NLO [15–17] can be formulated as:

$$\begin{aligned} \sigma = & F_{H_1}^g(x_1, \mu, m_c) F_{H_2}^g(x_2, \mu, m_c) \otimes \hat{\sigma}_{gg \rightarrow \Xi_{cc}(\bar{c}\bar{c})}(x_1, x_2, \mu, m_c) + \left\{ \sum_{i,j=1,2;i \neq j} F_{H_i}^g(x_i, \mu, m_c) [F_{H_j}^c(x_j, \mu, m_c) \right. \\ & \left. - F_{H_j}^c(x_j, \mu, m_c)_{\text{SUB}}] \otimes \hat{\sigma}_{g c \rightarrow \Xi_{cc}(\bar{c}\bar{c})}(x_1, x_2, \mu, m_c) \right\} + \left\{ \sum_{i,j=1,2;i \neq j} [(F_{H_i}^c(x_i, \mu, m_c) - F_{H_i}^c(x_i, \mu, m_c)_{\text{SUB}}) \right. \\ & \left. \cdot (F_{H_j}^c(x_j, \mu, m_c) - F_{H_j}^c(x_j, \mu, m_c)_{\text{SUB}})] \otimes \hat{\sigma}_{cc \rightarrow \Xi_{cc}(g)}(x_1, x_2, \mu, m_c) \right\} + \dots, \end{aligned} \quad (1)$$

²As stated above, here the so-called LO extrinsic charm fusion with the subprocesses $c + c \rightarrow (cc)[^3S_1]_{\mathbf{\bar{3}}}$ and $c + c \rightarrow (cc)[^1S_0]_{\mathbf{6}}$ are not taken into account, alternatively, the NLO mechanisms with the subprocesses: $c + c \rightarrow (cc)[^3S_1]_{\mathbf{\bar{3}}} + g$, $c + c \rightarrow (cc)[^1S_0]_{\mathbf{6}} + g$ are, so as to have a ‘‘complete the estimate’’. In order to guarantee pQCD applicable, we compute the production always to put on a sizable cut on the transverse momentum $p_t \simeq m_c$ of the produced (cc) -pair.

where the ellipsis means all the “other mechanisms” and higher order α_s terms. The “other mechanisms” include those of the light quark annihilations

$$\begin{aligned} & \sum_{q=u,d,s} F_{H_1}^q(x_1, \mu, m_c) F_{H_2}^{\bar{q}}(x_2, \mu, m_c) \\ & \times \bigotimes \hat{\sigma}_{q\bar{q} \rightarrow \Xi_{cc}[\bar{c}\bar{c}]}(x_1, x_2, \mu, m_c) \\ & + \sum_{q=u,d,s} F_{H_1}^{\bar{q}}(x_1, \mu, m_c) F_{H_2}^q(x_2, \mu, m_c) \\ & \times \bigotimes \hat{\sigma}_{\bar{q}q \rightarrow \Xi_{cc}[\bar{c}\bar{c}]}(x_1, x_2, \mu, m_c) \end{aligned}$$

and the LO extrinsic charm fusion mechanisms via the subprocesses $c + c \rightarrow (cc)[^3S_1]_3$ and $c + c \rightarrow (cc)[^1S_0]_6$, and etc. It is known from the experiences of B_c production estimates such as shown in Ref. [12] that the contributions from the light quark annihilation mechanisms are much smaller than those of gluon-gluon fusion (the first term of Eq. (1)). So, we do not consider them in this paper, and also we shall not consider the LO extrinsic charm fusion mechanisms for the reason stated in INTRODUCTION. Therefore, in Eq. (1) the “other mechanisms” are not included precisely. Note here, the third term of Eq. (1) in fact is the NLO extrinsic charm fusion mechanisms and to emphasize the using of GM-VFN scheme, the c -quark mass are explicitly put into both the PDFs and the hard-scattering kernel in Eq. (1). $F_H^i(x, \mu, m_c)$ (with $H = H_1$ or H_2 ; $x = x_1$ or x_2) is the distribution function of parton i in hadron H . Here $\hat{\sigma}$ stands for the cross-section of the corresponding subprocess. For convenience, we have taken the renormalization scale μ_R for the subprocess and the factorization scale μ_F for factorizing the PDFs and the hard subprocess to be the same, i.e. $\mu_R = \mu_F = \mu$. The subtraction for $F_H^c(x, \mu, m_c)$ is defined as

$$\begin{aligned} F_H^c(x, \mu, m_c)_{\text{SUB}} & \equiv F_H^g(x, \mu, m_c) \bigotimes F_g^c(x, \mu, m_c) \\ & = \int_x^1 \frac{dy}{y} F_g^c(y, \mu, m_c) F_H^g\left(\frac{x}{y}, \mu, m_c\right). \end{aligned} \quad (2)$$

The charm quark distribution $F_g^c(x, \mu, m_c)$ inside an on-shell gluon up to order α_s can be connected to the familiar $g \rightarrow c\bar{c}$ splitting function $P_{g \rightarrow c}$, i.e. $F_g^c(x, \mu, m_c) = \frac{\alpha_s(\mu)}{2\pi} \ln \frac{\mu^2}{m_c^2} P_{g \rightarrow c}(x)$, with $P_{g \rightarrow c}(x) = \frac{1}{2}(1 - 2x + 2x^2)$. Later on for convenience, we shall call the “heavy-quark mechanisms”, in which proper subtraction has been given according to method in GM-VFN scheme, as “extrinsic ones” accordingly.

In fact, Eq. (1) indicates that the “first step” of the hadronic production of Ξ_{cc} is about two charm quarks being produced inclusively, because it is based on non-relativistic QCD (NRQCD) formulation, and according to NRQCD, the production of the charm diquark (cc) is

factorized into “two steps”: producing two charm quarks first and then forming the diquark nonperturbatively. The transition of the produced two charm quarks into the (cc)-diquark is depicted in terms of NRQCD matrix elements [10]. At the leading order of v_c , the baryon Ξ_{cc} contains two configurations of the (cc)-diquark, one is that in $(cc)_3[^3S_1]$, another is that in $(cc)_6[^1S_0]$. The relevant matrix elements can be defined as

$$\begin{aligned} (cc)_6[^1S_0]: h_1 & \equiv \frac{1}{48} \langle 0 | [\psi^{a_1} \epsilon \psi^{a_2} + \psi^{a_2} \epsilon \psi^{a_1}] \\ & \times (a^\dagger a) \psi^{a_2^\dagger} \epsilon \psi^{a_1^\dagger} | 0 \rangle, \\ (cc)_3[^3S_1]: h_3 & \equiv \frac{1}{72} \langle 0 | [\psi^{a_1} \epsilon \sigma^i \psi^{a_2} - \psi^{a_2} \epsilon \sigma^i \psi^{a_1}] \\ & \times (a^\dagger a) \psi^{a_2^\dagger} \sigma^i \epsilon \psi^{a_1^\dagger} | 0 \rangle, \end{aligned} \quad (3)$$

where $a_j = 1, 2, 3$ ($j = 1, 2$) label the color of the valence quark fields, σ^i ($i = 1, 2, 3$) are Pauli matrices and $\epsilon = i\sigma^2$. h_1 represents the probability for that the possible diquark $(cc)_6[^1S_0]$ is formed by the two charm quarks, while h_3 represents the probability for that the possible diquark $(cc)_3[^3S_1]$ is formed by the two charm quarks. Both h_1 and h_3 are of order v_c^2 to $|\langle 0 | \chi^\dagger \sigma \psi | ^3S_1 \rangle|^2$ [9]. The value of the two matrix elements h_1 and h_3 can be determined with nonperturbative methods such as QCD sum rule approach, however their values are unknown yet. As the last step, the fragmentation of a diquark (cc) into the baryon Ξ_{cc} is assumed to occur with unit probability and consequently, to have no influence on the production cross section, namely to assume that the fragmentation function $D(z)$ of a heavy diquark into a baryon has a very sharp peak near $z \approx 1$ [6],³ and finally the momentum of the baryon may be considered roughly equal to the momentum of initial diquark. So to study the hadronic production of Ξ_{cc} is equivalent to study the hadronic production of (cc)-diquark. Under such condition, the value of NRQCD matrix element h_3 can be naively related to the wave-function for the color antitriplet [3S_1] cc state, i.e. $h_3 = |\Psi_{cc}(0)|^2$. And for convenience, since h_1 and h_3 is of the same order in v_c . We take h_1 equal to h_3 hereafter.

The schematic Feynman diagrams for the gluon-gluon fusion mechanism (corresponding to the first term in Eq. (1)) are shown in Fig. 1. There are two ways for the two outgoing charm quarks to form the (cc)-diquark and each contains 36 Feynman diagrams, while the 36 Feynman diagrams are similar to those for hadronic production of B_c (all the diagrams can be found in Ref. [19], but one needs to change all the b (\bar{b}) quark line there to the c (\bar{c}) quark line). However in Refs. [5–7], only Fig. 1(a) is considered and then only 36 Feynman diagrams have been

³By taking a simple form of fragmentation function $D(z)$, the authors of Ref. [7,18] did a rough estimation for such effects. Their results there indeed show that such effect is really small.

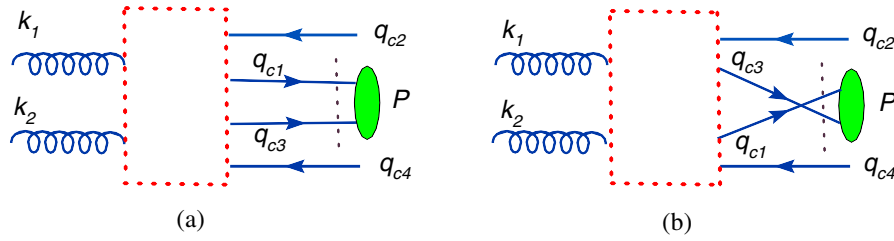


FIG. 1 (color online). The schematic Feynman diagrams of the gluon-gluon mechanism for the hadroproduction of Ξ_{cc} . The dashed box stands for the hard interaction kernel. k_1 and k_2 denote two momenta for the initial gluons, q_{c2} and q_{c4} denote the momenta for the two outgoing \bar{c} and P denotes the momentum of Ξ_{cc} . The (cc) -diquark is either in $(cc)_3[{}^3S_1]$ or in $(cc)_6[{}^1S_0]$ respectively.

taken into consideration. Since the contributions from the left and the right diagrams of Fig. 1 are the same and there is an $(\frac{1}{2})$ factor for the square of the amplitude by taking into account the symmetry of the diquark wave function. So, there is an overall factor “2” for our total cross-sections in comparing with those in Refs. [5–7]. In the present paper, as a cross check of the results in Refs. [5–7], we calculate the cross-sections by using two different methods. One method is to fully simplify the amplitude of the gluon-gluon fusion mechanism by using the improved helicity approach which was developed in case of the hadronic production of B_c [19,20]. More details of the calculation could be found in the appendix A. The other one is to generate the Fortran program directly by the Feynman Diagram Calculation (FDC) program [21], which is a Reduce and Fortran package to perform Feynman diagram calculation automatically. The detailed technique of Ξ_{cc} production in FDC can be found in Appendix B.

For the mechanisms relevant to the “extrinsic charm”, the typical Feynman diagrams are shown in Fig. 2 and 3. Fig. 2 is gluon-charm creation mechanism (corresponding to the second and the third terms in Eq. (1)) and Fig. 3 is NLO charm fusion mechanism with a real gluon emission (corresponding to the third terms in Eq. (1)). The final

expressions of the total square of amplitudes for the gluon-charm creation mechanism and the NLO charm fusion mechanism are comparatively simple, and we adopt the FDC program [21] to obtain them directly.

Here we calculate the “extrinsic” charm mechanism within the GM-VFN scheme. When one talks about the heavy-quark components of PDFs and summing up the contributions from the “heavy-quark mechanisms” and the gluon-gluon fusion mechanism for the hadronic production, one has to solve the double counting problem. A full QCD “heavy-quark” charm/bottom distribution function appearing in “heavy-quark mechanisms” includes all the terms proportional to $\ln(\frac{\mu^2}{m_Q^2})$ (μ the factorization scale and m_Q the heavy-quark mass); but some of them, in fact, just come from the subprocess of gluon-gluon fusion mechanism via the integration of the phase-space. Therefore, when summing up the contributions from the “heavy-quark mechanisms” and gluon-gluon fusion mechanism without proper subtraction, double counting happens.

To be specific in GM-VFN scheme, the inclusive Ξ_{cc} hadronic production is just formulated explicitly as Eq. (1) with proper subtraction terms $F_H^c(x, m_c, \mu)_{\text{SUB}}$ as defined

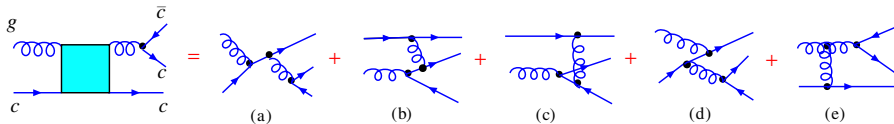


FIG. 2 (color online). Typical Feynman diagrams for the subprocesses $g(p_1) + c(p_2) \rightarrow c(k_1) + c(k_2) + \bar{c}(p_4)$, where $c(k_1)$ and $c(k_2)$ will form a diquark (cc) with the momentum of $p_3 = k_1 + k_2$.

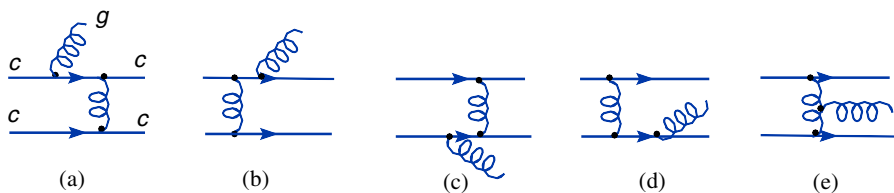


FIG. 3 (color online). Typical Feynman diagrams for the subprocesses $c(p_1) + c(p_2) \rightarrow c(k_1) + c(k_2) + g(p_4)$, where $k_1 + k_2 = p_3$ is the momentum of the final formed diquark (cc) .

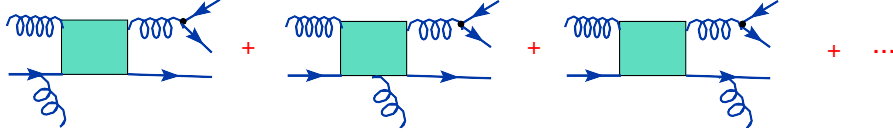


FIG. 4 (color online). Typical Feynman diagrams for the subprocesses $g + c \rightarrow c + c + \bar{c} + g$, which are of next-to-leading-order (the real correction of $g + c \rightarrow c + c + \bar{c}$).

in Eq. (2). The cross-sections corresponding to the 2-to-2 subprocesses $d\hat{\sigma}_{ij \rightarrow \Xi_{cc}}$ appearing in Eq. (1) stands as follows:

$$d\hat{\sigma}_{ij \rightarrow \Xi_{cc}}(x_1, x_2, m_c, \mu^2) = \frac{(2\pi)^4 |\bar{M}|^2}{4\sqrt{(p_1 \cdot p_2)^2 - m_1^2 m_2^2}} \times \prod_{i=3}^4 \frac{d^3 \mathbf{p}_i}{(2\pi)^3 (2E_i)} \times \delta\left(\sum_{i=3}^4 p_i - p_1 - p_2\right), \quad (4)$$

where p_1, p_2 are the corresponding momenta for the initial two partons, and p_3 is the momentum of the diquark (cc), p_4 is the momentum of gluon in the final state. The average over the initial parton's spins and colors, and the summation over the final state's spins and colors as well are absorbed into $|\bar{M}|^2$. The expression of $|\bar{M}|^2$, with all the mass effects being retained, is presented in Appendix B.

The phase-space integrations appearing in the numerical calculations are manipulated by adopting the routines RAMBOS [22] and VEGAS [23], which are also adopted in the B_c meson generator BCVEGPY [19,20].

In Ref. [17], the authors claimed that they obtained the “new matter” in addition to the ACOT scheme [15], i.e. for their concerned process they obtained the additional terms $f_A^c \otimes {}^1\omega_{c,\lambda}^{c,X} - f_A^c \otimes \tilde{f}_c^c \otimes {}^0\omega_{c,\lambda}^c$, which correspond to the virtual correction to the Born process $\gamma + c \rightarrow c$ and the real correction: $\gamma + c \rightarrow g + c$ accordingly. Thus in a similar way, the “new matter” for the present estimate would be that there are additional terms originated from the virtual correction of $g + c \rightarrow c + c + \bar{c}$ and the real correction (i.e. the terms for $g + c \rightarrow c + c + \bar{c} + g$ corresponding to the diagrams as shown in Fig. 4). Whereas, one may see that from the left figure of Fig. 4, the effects of the real and virtual corrections of $g + c \rightarrow c + c + \bar{c}$ are attributed to the PDFs corresponding under GM-VFN scheme, while the “survived effects” are of high order in comparison with the LO gluon-charm creation itself $g + c \rightarrow c + c + \bar{c}$. At present stage, we just restrict ourselves to re-estimate the production at LO, i.e. in the so-called ACOT approach [15] in a sense, so we drop them as our final result.

III. ON THE NUMERICAL CALCULATIONS

Before analyzing the properties for the hadronic production of Ξ_{cc} , we need to check the programs for numerical calculations, especially, we should take more care on the most complicate mechanism: gluon-gluon fusion.

First of all, we have checked all the programs by examining the gauge invariance of the amplitude, i.e. the amplitude vanishes when the polarization vector of an initial/final gluon is substituted by its momentum vector.⁴ Numerically, we find that the gauge invariance is guaranteed at the computer ability (double precision) for all the relevant subprocesses. Next, to make sure the correctness of our program for the gluon-gluon fusion mechanism, as mentioned before, the numerical results of our various programs agree with each other exactly.

Furthermore, we have compared our numerical results for the gluon-gluon fusion mechanism with those in literature by using the same input parameters. To make a complete comparison with the results listed in Ref. [5], we have also calculated the partonic cross sections for the production of Ξ_{bc} and Ξ_{bb} through the subprocesses, $gg \rightarrow \Xi_{bc} + \bar{b} + \bar{c}$ with the (bc) -diquark in color-anti-triplet [3S_1] or [1S_0] state, and $gg \rightarrow \Xi_{bb} + \bar{b} + \bar{b}$ with the (bb) -diquark in color-anti-triplet [3S_1] state. By the way, we note here that the programs for the production of Ξ_{bc} and Ξ_{bb} can be easily obtained from the program for the case of Ξ_{cc} .

In Fig. 5, we show the partonic cross sections for the production of baryons with heavy diquarks via the gluon-gluon fusion subprocess. In drawing the curves, we adopt the same parameter values as taken in Ref. [5], i.e. with a fixed value for α_s ($\alpha_s = 0.2$) and

$$|\Psi_{cc}(0)|^2 = 0.039 \text{ GeV}^3, \quad |\Psi_{bc}(0)|^2 = 0.065 \text{ GeV}^3, \\ |\Psi_{bb}(0)|^2 = 0.152 \text{ GeV}^3, \quad (5)$$

$$m_c = 1.8 \text{ GeV}, \quad m_b = 5.1 \text{ GeV}, \\ M_{\Xi_{cc}} = 3.6 \text{ GeV}, \quad M_{\Xi_{bc}} = 6.9 \text{ GeV}, \quad (6) \\ M_{\Xi_{bb}} = 10.2 \text{ GeV}.$$

For convenience of the comparison with those of Ref. [5], in Fig. 5 the curves of ours are that our results about Ξ_{cc} and Ξ_{bb} have been divided by an overall factor “2”. One

⁴All the Fortran codes are available from the authors on request.

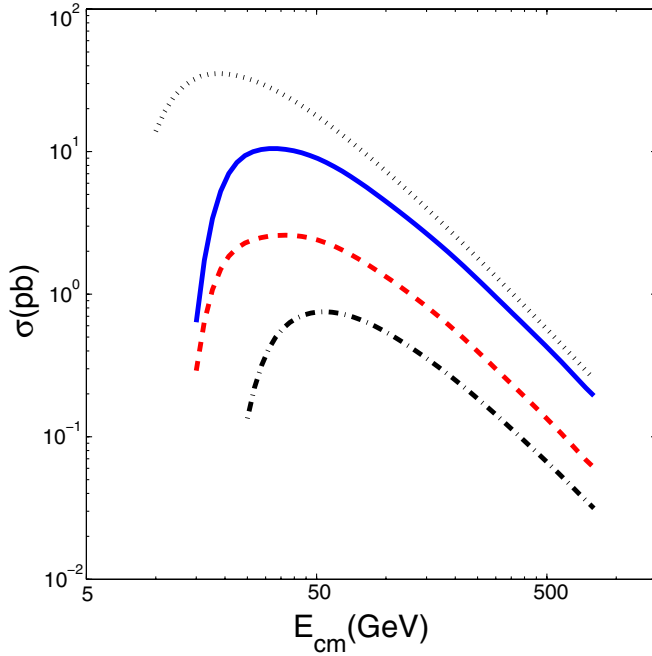


FIG. 5 (color online). The energy dependence of the integrated partonic cross-section for the production of the baryons via the heavy diquarks in terms of the gluon-gluon fusion mechanism. The dotted line, solid line, dashed line and dash-dot line stand for those via the diquarks $(cc)_3^3[{}^3S_1]$, $(bc)_3^3[{}^3S_1]$, $(bc)_3^1[{}^1S_0]$ and $(bb)_3^3[{}^3S_1]$ respectively. The curves for Ξ_{cc} and Ξ_{bb} both are divided by 2.

may easily find all the curves for the energy dependence of the partonic cross-sections shown in Fig. 5 are in consistent with the results in Fig. 2a of Ref. [5]. Namely our results are 2 times of those in Ref. [5], and we suspect that the difference is due to identical particle counting for the diquark (cc) and (bb) .

In Table I, we show the comparison of partonic cross sections (the second column) for the production of Ξ_{cc} via the (cc) -diquark in $(cc)_3^3[{}^3S_1]$ in terms of the gluon-gluon fusion subprocess as those in Refs. [6,7]. In Table I, the results of Ref. [6] is derived from the fitted expression (Eq. (8) in Ref. [6]):

$$\sigma = 213. \left(1 - \frac{4m_c}{E_{\text{cm}}}\right)^{1.9} \left(\frac{4m_c}{E_{\text{cm}}}\right)^{1.35}, \quad (7)$$

TABLE I. Comparison of the partonic cross sections for $gg \rightarrow \Xi_{cc} + \bar{c} + \bar{c}$ with the corresponding results in Ref. [6], where the (cc) -diquark is in $(cc)_3^3[{}^3S_1]$. E_{cm} is the center of mass energy of the subprocess. The input parameters are $m_c = 1.7$ GeV, $M_{\Xi_{cc}} = 3.4$ GeV, the radial wave function at the origin $R_{cc}(0) = \sqrt{4\pi}\Psi_{cc}(0) = 0.601$ GeV $^{3/2}$ and $\alpha_s = 0.2$.

E_{cm}	15 GeV	20 GeV	40 GeV	60 GeV	80 GeV	100 GeV
$\sigma(pb)$	66.6	68.2	41.8	26.2	17.9	13.1
$\sigma(pb)$ [6]	23.2	22.5	13.7	8.96	6.45	4.94

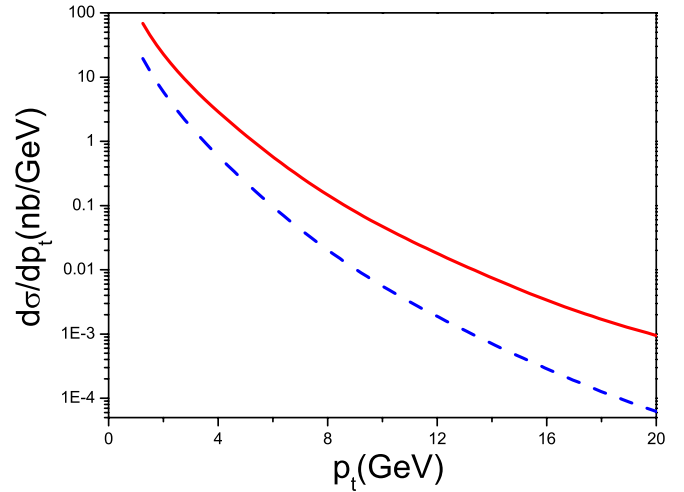


FIG. 6 (color online). The p_t -distributions for the ‘‘extrinsic’’ mechanism $c + c \rightarrow \Xi_{cc} + g$ at Tevatron RUN-I $E_{\text{cm}} = 1.8$ TeV (dashed line) and at LHC $E_{\text{cm}} = 14$ TeV (solid line) both with $|y| \leq 1.0$. The present results are calculated with the same parameters in Ref. [18].

where E_{cm} is the center of mass energy of the subprocess. One may observe that under the same parameter values, the results in Refs. [6,7] are in disagreement with ours⁵.

Next, as a cross check between our results for the ‘‘extrinsic’’ mechanism through the subprocess $c + c \rightarrow \Xi_{cc} + g$ with those in Ref. [18], we show the cross section of Ξ_{cc} -baryon production at the hadronic energy $E_{\text{cm}} = 1.8$ TeV or 14 TeV with the same input parameters as in Fig. 6. The curves in Fig. 6 indeed agree with the figures Figs. 3,4 of Ref. [18].

As a summary, for the gluon-gluon fusion mechanism, except for an overall factor ‘‘2’’, we confirm the results in Ref. [5], but not those of Ref. [6,7]. And for one of the ‘‘extrinsic’’ charm mechanism, i.e. considering the subprocess $c + c \rightarrow \Xi_{cc} + g$ itself, our results agree with those of Ref. [18] under the same input parameters.

Finally, we discuss the properties of the two different configurations of (cc) -diquark, i.e. $(cc)_3^3[{}^3S_1]$ and $(cc)_6^1[{}^1S_0]$, for the hadronic production of Ξ_{cc} . In Fig. 7, we show the transverse momentum P_t distribution and the rapidity y distribution at different center-mass energies for the subprocess $gg \rightarrow \Xi_{cc} + \bar{c} + \bar{c}$, with (cc) -diquark in $(cc)_3^3[{}^3S_1]$. The case is similar for (cc) -diquark in $(cc)_6^1[{}^1S_0]$ that is not shown here. In Fig. 8 we draw curves to present the energy dependence of the integrated partonic cross-sections, so as to have a comparison between the two different (cc) -diquark configurations $(cc)_3^3[{}^3S_1]$ and $(cc)_6^1[{}^1S_0]$. One may observe that the curves for $(cc)_3^3[{}^3S_1]$ and $(cc)_6^1[{}^1S_0]$ are similar in shape and the

⁵Such discrepancy has already been found in Ref. [5], however the author there attribute it to the different use of input parameters.

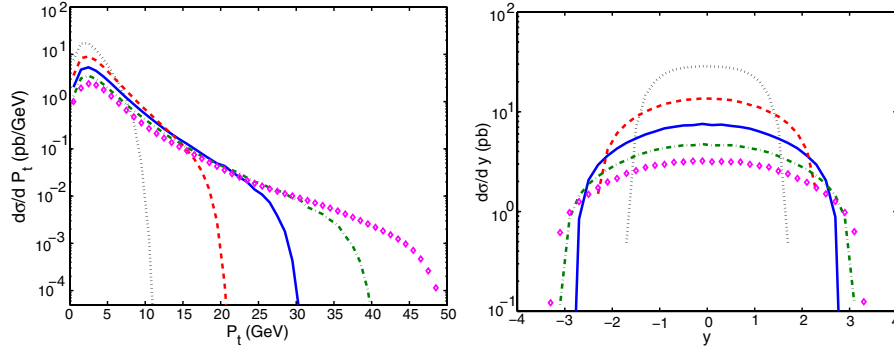


FIG. 7 (color online). The P_t - and y -distributions of the produced Ξ_{cc} for the subprocess $gg \rightarrow \Xi_{cc} + \bar{c} + \bar{c}$ under different C.M. energies. Here the diquark only in $(cc)_3[{}^3S_1]$ is taken into account. The dotted line, dashed line, solid line, dash-dot line and the diamond line stand for $E_{cm} = 20$ GeV, 40 GeV, 60 GeV, 80 GeV and 100 GeV, respectively.

contributions from $(cc)_6[{}^1S_0]$ can be greater than those from $(cc)_3[{}^3S_1]$ by a factor $\sim 20\%$. So the contributions from the (cc) -diquark $(cc)_6[{}^1S_0]$ should be taken into account for the estimation of the hadronic production of Ξ_{cc} because they are sizable. This is in agreement with the conclusion drawn in Ref. [9], where the contributions from these two different states of (cc) -diquarks are discussed through the fragmentation approach.

IV. HADRONIC PRODUCTION OF Ξ_{cc}

In the present section, we shall first study the hadronic production properties of Ξ_{cc} at colliders TEVATRON and LHC, and then discuss the hadronic production at the fixed target SELEX experiment. All the calculations in the section are done under the GM-VFN scheme as stated in Sec. II.

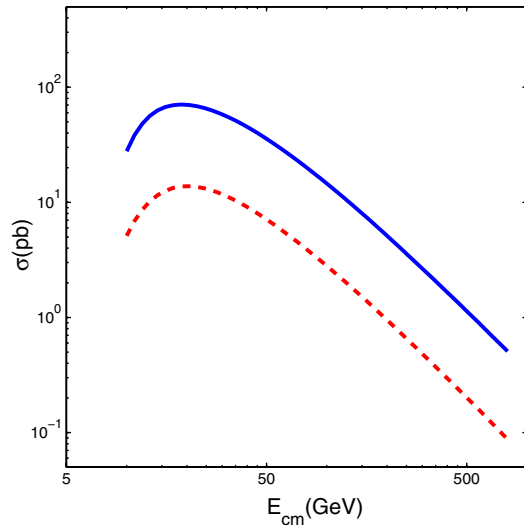


FIG. 8 (color online). The energy dependence of the integrated partonic cross-section for the Ξ_{cc} production of via the gluon-gluon fusion mechanism. The solid line and the dashed line stand for the two (cc) -diquark states in configurations $(cc)_3[{}^3S_1]$ and $(cc)_6[{}^1S_0]$ respectively.

As stated in Sec. II, in the calculations we take $h_3 = |\Psi_{(cc)}(0)|^2$ and $h_1 = h_3$. The mass of diquark $M_{(cc)}$ can be obtained by potential model, and the mass of Ξ_{cc} baryon, $M_{\Xi_{cc}}$, can be estimated by $M_{\Xi_{cc}} \simeq M_{(cc)} + m_q$ (m_q is the pole mass of light quark q) to be $M_{\Xi_{cc}} \simeq 3.584 \pm 0.035$ GeV [6]. In Ref. [1], it has been measured to be 3.519 ± 0.001 GeV. The effective c -quark mass can be derived from the value of the pole mass and the relation between the pole mass and the \overline{MS} running mass [24]. For clarity, we choose $|\Psi_{(cc)}(0)|^2 = 0.039$ GeV³ [5], $M_{\Xi_{cc}} = 3.50$ GeV and with $m_c^{\text{eff}} = 1.75$ GeV. The factorization energy scale is fixed to be the transverse mass of Ξ_{cc} , i.e. $\mu = M_t \equiv \sqrt{M^2 + p_t^2}$, where p_t is the transverse momentum of the baryon. The PDFs of version CTEQ6HQ [13] and the leading order α_s running above $n_f = 4$ with $\Lambda_{\text{QCD}}^{(n_f=4)} = 0.215$ GeV are adopted. Since the calculated hard-scattering kernel is of leading order, so strictly, we need to take a leading-order PDFs for the initial parton distributions such as CTEQ6L1 [25]. However under GM-VFN scheme, the so-called NLO PDFs are needed, which can be found in version CTEQ6HQ. At TEVATRON or LHC for the hadronic production, where a large p_t cut, e.g. $p_t > 4$ GeV, is introduced, PDFs from the different versions CTEQ6HQ or CTEQ6L1 just cause one kind of theoretical uncertainties (it is similar for estimate of the hadronic production of the doubly heavy B_c meson [12]). Such different use of the PDF mainly causes the discrepancy in small p_t regions so do not affect the final results at TEVATRON or LHC too much. While for the hadronic production at SELEX, the situation is different, since it can reach to a region of much smaller p_t , so much more careful treatment should be made and we shall discuss the uncertainty caused by the different type of PDF in the Sec. IV C.

A. Hadronic production of Ξ_{cc} at colliders LHC and TEVATRON

In Table II, we show the cross-sections for the hadronic production of Ξ_{cc} at colliders TEVATRON and LHC with

TABLE II. Cross sections (σ) for the hadronic production of Ξ_{cc} at colliders TEVATRON and LHC, where the (cc) -diquark is in $(cc)_3^3[{}^3S_1]$ or $(cc)_6^1[{}^1S_0]$, and the symbol $g + c$ means $g + c \rightarrow \Xi_{cc} + \bar{c}$ and etc. In the calculations, cuts $p_t \geq 4$ GeV and $|y| \leq 1.5$ are taken at LHC, while at TEVATRON cuts $p_t \geq 4$ GeV, $|y| \leq 0.6$ instead.

	TEVATRON ($\sqrt{s} = 1.96$ TeV)		LHC ($\sqrt{s} = 14.0$ TeV)	
	$(cc)_3^3[{}^3S_1]$	$(cc)_6^1[{}^1S_0]$	$(cc)_3^3[{}^3S_1]$	$(cc)_6^1[{}^1S_0]$
$\sigma_{g+g}(nb)$	1.61	0.392	22.3	5.44
$\sigma_{c+g}(nb)$	2.29	0.360	22.1	3.42
$\sigma_{c+c}(nb)$	0.751	0.0431	8.74	0.475

proper p_t - and y -cut. From Table II, one may observe that similar to the case of hadronic production of B_c meson [12], the cross-sections of the ‘‘extrinsic’’ charm mechanisms are comparable to, or even bigger than, the usual considered gluon-gluon fusion mechanism. One may also observe that the contributions from $(cc)_6^1[{}^1S_0]$ are sizable comparing with that of $(cc)_3^3[{}^3S_1]$, i.e. for the gluon-gluon fusion mechanism, the contribution from $(cc)_6^1[{}^1S_0]$ is about 24% of that of $(cc)_3^3[{}^3S_1]$, while for the mechanisms of $c + g \rightarrow \Xi_{cc} + \bar{c}$ and $c + c \rightarrow \Xi_{cc} + 'g'$, it is about $\sim 15\%$ and $\sim 5\%$, respectively.

In Fig. 9, we show p_t -distributions for the hadronic production of Ξ_{cc} with two configurations of the (cc) -diquark states, i.e. $(cc)_3^3[{}^3S_1]$ and $(cc)_6^1[{}^1S_0]$, where $|y| \leq 1.5$ at LHC and $|y| \leq 0.6$ at TEVATRON are adopted. From Fig. 9, one may observe the following points: (i) to compare with the gluon-gluon fusion mechanism, the ‘‘extrinsic’’ mechanism $g + c \rightarrow \Xi_{cc} + 'g'$ dominant in small p_t regions and its p_t -distribution drops faster than that of gluon-gluon fusion mechanism, which is similar to the case of B_c hadroproduction [12]. (ii) For ‘‘extrinsic’’ mechanism $c + c \rightarrow \Xi_{cc} + 'g'$, the p_t -distribution drops faster than other mechanisms and then its contribution is the smallest among all the mechanisms. (iii) For each mechanism, the contribution from $(cc)_6^1[{}^1S_0]$ is smaller but sizable in comparison with the

contribution from $(cc)_3^3[{}^3S_1]$. From Fig. 9, one may see the feature that in the whole p_t regions, the p_t -distribution of $(cc)_6^1[{}^1S_0]$ is smaller than that of $(cc)_3^3[{}^3S_1]$ for the same mechanism and it also drops faster than the case of $(cc)_3^3[{}^3S_1]$. Especially for the $c + c \rightarrow \Xi_{cc} + 'g'$ mechanism, p_t -distribution of $(cc)_6^1[{}^1S_0]$ drops much faster than that of $(cc)_3^3[{}^3S_1]$, and then the cross-section for $(cc)_6^1[{}^1S_0]$ is only about 5% of that of $(cc)_3^3[{}^3S_1]$. As for the gluon-gluon fusion mechanism, the contribution from $(cc)_6^1[{}^1S_0]$ is comparable to that of $(cc)_3^3[{}^3S_1]$ from the ‘‘extrinsic’’ mechanisms at high energies, especially at LHC, so one should take the contribution from $(cc)_6^1[{}^1S_0]$ into account also if one wishes to have a complete estimate of the production via all these hadronic mechanisms.

B. Hadronic production of Ξ_{cc} at the fixed target SELEX experiment

For a fixed target experiment of SELEX, the ‘‘extrinsic’’ charm mechanisms of hadronic production become more important than that at TEVATRON or LHC, since small p_t events can contribute. Such an experiment may cover all solid angle almost without p_t cut, thus the ‘‘extrinsic’’ charm mechanisms may be studied and extended to very small p_t region. For SELEX experiment [1], its lower p_t bound can be so small as 0.2 GeV. However, to make an estimate for SELEX, one should ensure that the pQCD calculation is applicable in such small p_t regions, i.e. the gluon (with momentum q) in all the mechanisms for the hadronic production of Ξ_{cc} must be hard enough, i.e. $q^2 \gg \Lambda_{\text{QCD}}^2$.

For the gluon-gluon fusion subprocess to produce $c\bar{c}$ -quark pairs, the square of the gluon momentum q^2 at least is bigger than $4m_c^2 \gg \Lambda_{\text{QCD}}^2$ so the subprocess is always pQCD calculable. For the ‘‘extrinsic’’ subprocess $g(p_1) + c(p_2) \rightarrow \Xi_{cc}(p_3) + \bar{c}(p_4)$ depicted by Figs. 2(a) and 3(b)–3(d), obviously, the momentum q of the intermediate gluon appearing in Figs. 2(a) and 2(d) has $q^2 \geq 4m_c^2 \gg \Lambda_{\text{QCD}}^2$, moreover, we may also ensure by precise

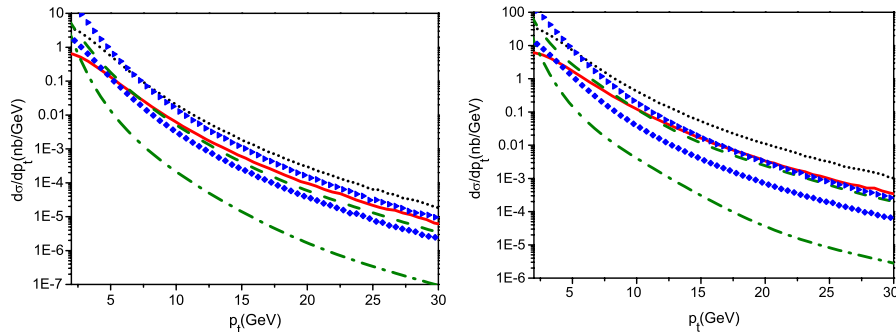


FIG. 9 (color online). The p_t -distribution for the hadroproduction of Ξ_{cc} at TEVATRON (left) and at LHC (right), where $|y| \leq 1.5$ at LHC and $|y| \leq 0.6$ at TEVATRON are adopted. The dotted line and the solid line are for gluon-gluon fusion mechanism, the triangle line and the diamond line are for $g + c \rightarrow \Xi_{cc} + \bar{c}$, the dashed line and the dash-dot line are for $c + c \rightarrow \Xi_{cc} + 'g'$, where the upper lines of each mechanism are for $(cc)_3^3[{}^3S_1]$ and the lower lines are for $(cc)_6^1[{}^1S_0]$, respectively.

TABLE III. Cross section (σ) for the hadronic production of Ξ_{cc} at the fixed target experiment with center of mass energy 33.58 GeV, where the (cc) -diquark is in $(cc)_3[{}^3S_1]$ or $(cc)_6[{}^1S_0]$, and the symbol $g + c$ means $g + c \rightarrow \Xi_{cc} + \bar{c}$ and etc. In the calculations, $p_t > 0.2$ GeV is taken.

SELEX ($\sqrt{s} = 33.58$ GeV)			
	$\sigma_{g+c}(pb)$	$\sigma_{g+c}(pb)$	$\sigma_{c+c}(pb)$
$(cc)_3[{}^3S_1]$	4.03	102	1.02×10^{-3}
$(cc)_6[{}^1S_0]$	0.754	11.3	4.15×10^{-5}

estimate that the momentum q of the intermediate gluon appearing in Figs. (2(b), 2(c), and 2(e)) are satisfy

$$Q^2 \equiv -q^2 = -\left(p_1 - \frac{p_3}{2}\right)^2 \geq 0.5 m_c^2 \Lambda_{\text{QCD}}^2. \quad (8)$$

However, for the ‘‘extrinsic’’ subprocess $c(p_1) + c(p_2) \rightarrow \Xi_{cc}(p_3) + 'g'(p_4)$ (Fig. 3), contrarily, to be pQCD calculable, we must put on additional constraints on the momentum q of the intermediate gluon appearing in Fig. 3 as follows:

$$Q_1^2 \equiv -q_1^2 = -\left(p_1 - \frac{p_3}{2}\right)^2 \gg \Lambda_{\text{QCD}}^2, \quad (9)$$

$$Q_2^2 \equiv -q_2^2 = -\left(p_2 - \frac{p_3}{2}\right)^2 \gg \Lambda_{\text{QCD}}^2.$$

Equations in Eq. (9) give two extra constraints for both the partonic fractions x_1, x_2 and p_t . For definiteness in numerical calculations, we set the lowest values for Q^2, Q_1^2 and Q_2^2 to be $m_c^2 (\gg \Lambda_{\text{QCD}}^2)$.⁶

The cross-sections obtained by the estimate for the hadronic production of Ξ_{cc} at SELEX experiment are presented in Table III, where $p_t > 0.2$ GeV is adopted. Table III shows that at SELEX, the ‘‘extrinsic’’ charm mechanism is the dominant mechanism and then the theoretical predictions of Ξ_{cc} events at SELEX can be raised by more than an order. The p_t -distributions for the fixed target experiment are presented in Fig. 10. One may observe that the p_t -distributions of ‘‘extrinsic’’ mechanisms $g + c \rightarrow \Xi_{cc} + \bar{c}$ are bigger than that of the gluon-gluon fusion mechanism almost in all the p_t region, that is the reason why the total cross-section of $g + c \rightarrow \Xi_{cc} + \bar{c}$ mechanism is much larger than that of the gluon-gluon fusion mechanism as shown in Table III. For ‘‘extrinsic’’ mechanism $c + c \rightarrow \Xi_{cc} + 'g'$, its p_t -distribution starts at ~ 5 GeV due to the constraint Eq. (9) and its contribution is quite small. From Table III, one may also observe that the contributions from $(cc)_6[{}^1S_0]$ are also sizable comparing with those from $(cc)_3[{}^3S_1]$, that is similar to the hadronic production at colliders TEVATRON and LHC as shown in Table II, i.e. for the gluon-gluon fusion mecha-

⁶Since the restrict Q_1^2 and Q_2^2 to be $m_c^2 (\gg \Lambda_{\text{QCD}}^2)$ is put on, so we denote the subprocess as $c(p_1) + c(p_2) \rightarrow \Xi_{cc}(p_3) + 'g'(p_4)$ instead of $c(p_1) + c(p_2) \rightarrow \Xi_{cc}(p_3) + g(p_4)$ (without the restrict) in the paper.

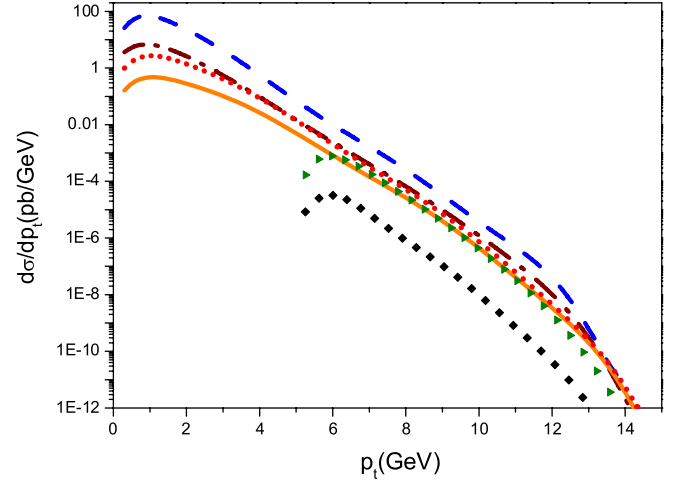


FIG. 10 (color online). The p_t -distributions for the hadroproduction of Ξ_{cc} at SELEX. The dotted line and the solid line are for gluon-gluon fusion mechanism, the dashed line and the dash-dot line are for $g + c \rightarrow \Xi_{cc} + \bar{c}$, the triangle line and the diamond line are for $c + c \rightarrow \Xi_{cc} + 'g'$, where the upper lines of each mechanism are for $(cc)_3[{}^3S_1]$ and the lower lines are for $(cc)_6[{}^1S_0]$, respectively.

nism, the contributions from $(cc)_6[{}^1S_0]$ are about 19% of those from $(cc)_3[{}^3S_1]$, while for the processes of $c + g \rightarrow \Xi_{cc} + \bar{c}$ and $c + c \rightarrow \Xi_{cc} + 'g'$, the situation changes about to $\sim 10\%$ and $\sim 4\%$, respectively.

C. Discussions on the estimate of the hadronic production at SELEX

The uncertainties in estimating the hadronic production of Ξ_{cc} at TEVATRON or LHC are caused by the parameters, such as the value of m_c , the matrix elements h_1 and h_3 , the factorization/renormalization scale μ , the PDFs and etc., which are similar to the case of the hadronic production of the double heavy meson B_c [26]. In this subsection, we will only concentrate on the uncertainties caused by the different choices of factorization/renormalization scale and the types of PDFs at SELEX. Varying the factorization/renormalization scales in a certain range would give us an idea on the higher order contributions in the estimate. And by studying the uncertainties caused by different PDFs will show us to what degree it will affect the final results.

For clarity, we take the factorization scale and the renormalization scale to be the same $\mu = \mu_F = \mu_R$ and take three choices for μ , i.e. $\mu = M_t$ (the default one in our calculations and $M_t \equiv \sqrt{M^2 + p_t^2}$), $\mu = 2M_t$ and $\mu = M_t/2$. The energy scale dependence of the summed p_t -distributions for each mechanism are shown in Fig. 11, where the contributions from $(cc)_3[{}^3S_1]$ and $(cc)_6[{}^1S_0]$ are summed up for each mechanism. Numerically, one may find that by taking $\mu = M_t/2$ (or $\mu = 2M_t$), the integrated cross-sections of the gluon-gluon fusion mechanism, the $g + c \rightarrow \Xi_{cc}$ mechanism and the

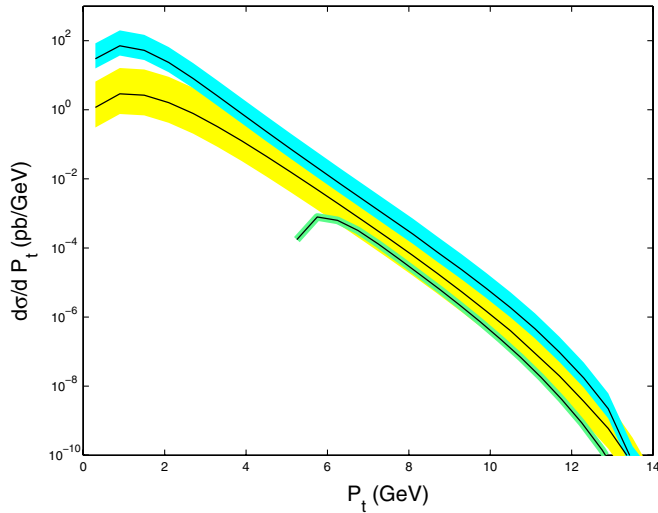


FIG. 11 (color online). The energy scale dependence of the p_t -distributions for each mechanism at SELEX, where the contributions from $(cc)_3[{}^3S_1]$ and $(cc)_6[{}^1S_0]$ are summed up. The upper band is for the mechanism $g + c \rightarrow \Xi_{cc}$, the middle band is for gluon-gluon fusion mechanism and the lower band is for $c + c \rightarrow \Xi_{cc}$ mechanism, where the solid line in each band corresponds to $\mu = M_t$, the upper edge of the band is for $\mu = M_t/2$ and the lower edge is for $\mu = 2M_t$, respectively.

$c + c \rightarrow \Xi_{cc}$ mechanism will be increased (or decreased) by ~ 5 , ~ 2.5 and ~ 1.5 times to the case of $\mu = M_t$, respectively.

As for the uncertainties from PDFs, we take CTEQ6HQ to do our calculations under the GM-VFN scheme. Strictly, it is inconsistent to use the version CTEQ6HQ here, since it is of next-to-leading order and is scheme dependent [13]. To be consistent, one need to calculate the hard-scattering kernel up to next-to-leading.⁷ By taking a leading-order PDF as CTEQ6L1 [25] (also inconsistent, since it is derived under the zero-mass variable-flavor-number scheme), we recalculate all the curves at SELEX and make a comparison with those of CTEQ6HQ in Fig. 12. Such calculations give us an impression on the inconsistent use of PDF. Fig. 12 shows that the results do not be affected too much by inputting different PDFs, i.e. the difference caused by adopting CTEQ6HQ or CTEQ6L is less than 30% of that of CTEQ6HQ. Of the two kinds of the uncertainties sources discussed here, the most important one is the factorization/renormalization scale.

By taking into account the “extrinsic“ mechanisms, the theoretical prediction on the Ξ_{cc} production can be raised by almost one order in comparison with the previous predictions in which only the gluon-gluon fusion mechanism is considered. Nevertheless, there is still a big discrepancy between the SELEX observation [1] and pQCD predictions. The used PDFs above are determined empiri-

⁷A next-leading-order calculation on this issue is in preparation [27].

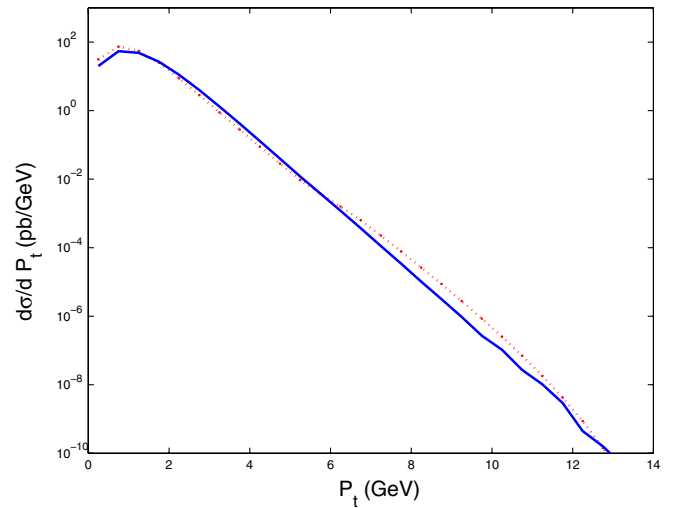


FIG. 12 (color online). p_t -distributions of the production for SELEX, obtained by using CTEQ6HQ and CTEQ6L1. The contributions from the gluon-gluon fusion and the extrinsic mechanisms, and via the two configurations of diquarks $(cc)_3[{}^3S_1]$ and $(cc)_6[{}^1S_0]$ are summed up. The dotted line is for CTEQ6HQ and the solid line is for CTEQ6L1.

cally by global fitting of the experimental data, where it is assumed that the charm content of the proton is negligible at $\mu \sim m_c$, and similarly that bottom is negligible at $\mu \sim m_b$, so these heavy-quark components arise only perturbatively through gluon splitting in the DGLAP evolution. As argued in Ref. [28], in obtaining the PDFs, even though the global fits are not inconsistent with this assumption, the data sets, used for the fits, do not yet include the experiments that are strongly sensitive to heavy quarks, so substantially sizable c or b content in the proton cannot be ruled out. The possibility of a sizable “intrinsic“ charm component in the nucleon wave function [14,28,29] might help to fill up the gap between the theoretical predictions and the experimental data of SELEX.

V. SUMMARY

We have calculated the hadronic production of the doubly charmed baryon Ξ_{cc} via the gluon-gluon fusion mechanism and the “extrinsic“ charm mechanism, i.e. via the subprocesses $g + g \rightarrow \Xi_{cc} + \dots$, $g + c \rightarrow \Xi_{cc} + \dots$ and $c + c \rightarrow \Xi_{cc} + \dots$ in the GM-VFN scheme in which the heavy-quark mass effects can be treated in a consistent way both for the hard-scattering amplitude and the PDFs. Some checks with those in literature have been done. The result for the gluon-gluon fusion mechanism agree with that given in Ref. [5] up to a factor of 2; and the results for the $c + c \rightarrow \Xi_{cc} + 'g'$ with (cc) -diquark in $(cc)_3[{}^3S_1]$ agree with that of Ref. [18] when taking the same input parameters. Whereas the results for the “extrinsic“ mechanisms and those for the cases with (cc) -diquark in $(cc)_6[{}^1S_0]$ are new.

From Table II and III, one may see that the total cross sections of the ‘‘extrinsic’’ charm mechanisms are comparable to, or even bigger than, that of the gluon-gluon fusion process, especially for the $g + c \rightarrow \Xi_{cc} + \bar{c}$ mechanism. To be more definite, we define a ratio

$$R = \frac{\sigma_{\text{total}}}{\sigma_{gg \rightarrow \Xi_{cc}((cc)_3[{}^3S_1])}}, \quad (10)$$

where σ_{total} stands for the cross section for all the concerned mechanisms and $\sigma_{gg \rightarrow \Xi_{cc}((cc)_3[{}^3S_1])}$ is the cross section for the gluon-gluon fusion mechanism with (cc) -diquark in $(cc)_3[{}^3S_1]$ configuration only. The values of R for the hadronic production of Ξ_{cc} in various environments are shown in Table IV, which shows that the ‘‘extrinsic’’ charm mechanisms are not negligible: at SELEX they even dominate over the other mechanisms. The contributions from the (cc) -diquark in $(cc)_6[{}^1S_0]$ for all the concerned mechanisms are also considered in this work, and the results show that if the matrix element h_1 is at the same order of h_3 [9], i.e. $h_1 \simeq h_3$, the diquark in $(cc)_6[{}^1S_0]$ contributes to the hadronic production of Ξ_{cc} sizably.

We may conclude that to be a complete estimation for the hadronic production of Ξ_{cc} , especially to extend the transverse momentum p_t as low as possible, one needs to take all of the mechanisms into account. One may observe that by taking into account the ‘‘extrinsic’’ mechanisms and by covering very small p_t , the theoretical prediction on the Ξ_{cc} events can be almost one order higher than the previous predictions in which only the gluon-gluon fusion mechanism is considered and only the events with a comparatively big p_t -cut are taken into account. Nevertheless, there is still a big discrepancy between the SELEX observation [1] and pQCD predictions. Perhaps it is due to the fact that the production in small p_t region is not amenable to the pQCD analysis, and being nonperturbative QCD nature, it is not considered here, but great enough to fill up the big discrepancy between the SELEX observation and the pQCD predictions, e.g., the ‘‘extrinsic’’ mechanism $c + c \rightarrow (cc)[{}^3S_1]_3 + g$ and $c + c \rightarrow (cc)[{}^1S_0]_6 + g$ as well as the extrinsic charm fusion mechanism with the subprocesses $c + c \rightarrow (cc)[{}^3S_1]_3$ and $c + c \rightarrow (cc)[{}^1S_0]_6$ contribute to the production greatly in small p_t region, however since they are out of the constraint Eq. (9) and are of nonperturbative nature, so they are not taken into account at all. Another possibility might be that the

TABLE IV. R values, which is defined in Eq. (10), for the hadronic production of Ξ_{cc} .

	SELEX	TEVATRON	LHC
- $p_t > 0.2$ GeV		$p_t \geq 4$ GeV, $ y \leq 0.6$	$p_t \geq 4$ GeV, $ y \leq 1.5$
R	29	3.4	2.8

SELEX group does not provide sufficient support for their claim of the evidence about doubly charmed baryon Ξ_{cc} as pointed out by Ref. [3].

ACKNOWLEDGMENTS

This work was supported in part by the Natural Science Foundation of China (NSFC). X.-G. Wu thanks the support from the China Postdoctoral Science Function.

APPENDIX A: CALCULATION TECHNOLOGY FOR THE GLUON-GLUON FUSION MECHANISM UNDER THE IMPROVED HELICITY APPROACH

The general structure of the amplitude in ‘‘explicit helicity’’ form can be written as

$$M_i^{(\lambda_2, \lambda_4, \lambda_5, \lambda_6)}(q_{c3}, q_{c4}, q_{c1}, q_{c2}, k_1, k_2) = g_s^4 \sum_{\lambda_2, \lambda_3} C_i X_i D_1 B_{Fi}^{(\lambda_1, \lambda_2, \lambda_3, \lambda_4, \lambda_5, \lambda_6)}(q_{c3}, q_{c4}, q_{c1}, q_{c2}, k_1, k_2) \cdot D_2 B_{(cc)}^{(\lambda_1, \lambda_3)}(q_{c3}, q_{c1}), \quad (A1)$$

where $i = 1, \dots, 72$, λ_j ($j = 1, \dots, 6$) denote the helicities of the quarks and gluons, respectively. λ_1 denotes the helicity of $c(q_{c3})$, λ_2 that of $\bar{c}(q_{c4})$, λ_3 that of $c(q_{c1})$, λ_4 that of $\bar{c}(q_{c2})$; whereas λ_5 denotes that of gluon-1 and λ_6 denotes that of gluon-2. Here C_i , X_i denote the color factor and the scalar factor from all the propagators as a whole for the i -th diagram, respectively. $B_{Fi}^{(\lambda_1, \lambda_2, \lambda_3, \lambda_4, \lambda_5, \lambda_6)}(q_{c3}, q_{c4}, q_{c1}, q_{c2}, k_1, k_2)$ and $B_{(cc)}^{(\lambda_1, \lambda_3)}(q_{c3}, q_{c1})$ are the amplitudes corresponding to the ‘‘free quark part’’ $g(k_1, \lambda_5)g(k_2, \lambda_6) \rightarrow c(q_{c3}, \lambda_1) + \bar{c}(q_{c4}, \lambda_2) + c(q_{c1}, \lambda_3) + \bar{c}(q_{c2}, \lambda_4)$ (all the quarks are on-shell) and the ‘‘bound state part’’ $c(q_{c3}, \lambda_1) + c(q_{c1}, \lambda_3) \rightarrow (cc)$, respectively. $D_1 = \frac{1}{\sqrt{2q_{c3} \cdot q_0}} \frac{1}{\sqrt{2q_{c4} \cdot q_0}} \frac{1}{\sqrt{2q_{c1} \cdot q_0}} \frac{1}{\sqrt{2q_{c2} \cdot q_0}}$ and $D_2 = \frac{1}{\sqrt{2q_{c1} \cdot q_0}} \frac{1}{\sqrt{2q_{c3} \cdot q_0}}$ are two common normalization factors.

By comparing Eq. (A1) with Eq. (22) in Ref. [19] that is for the B_c hadroproduction, one may observe that both amplitudes are quite similar with each other. Most of the present helicity amplitudes can be directly derived from the results in Ref. [19] by simply replacing the b -quark line there to the present c -quark line. And for the present case, we only need to deal with the following type of the helicity matrix element (HME) that is quite different from the case of B_c hadroproduction, i.e.

$$\text{HME}_i = \langle q_{0\lambda_2} | (\not{q}_{c4} + m_c) \hat{\Gamma}_i (\not{q}_{c3} - m_c) | q_{0\lambda_1} \rangle, \quad (A2)$$

where $i = (1, \dots, 72)$ stands for the i -th Feynman diagram and $\hat{\Gamma}_i$ means that all the momentum in Γ_i (Γ_i stands for the explicit strings of Dirac γ matrices between $\bar{U}(q_{c3})$ and $V(q_{c4})$, which corresponds to i -th Feynman diagram) should change their sign and the string of the γ -matrices in Γ_i should be written in inverse order. In fact, such type of

HME can also relate to the familiar one as has been dealt with in the B_c case by adopting the following relation:

$$\text{HME}_i = -\langle q_{0(-\lambda_1)} | (\not{q}_{c3} + m_c) \Gamma_i (\not{q}_{c4} - m_c) | q_{0(-\lambda_2)} \rangle. \quad (\text{A3})$$

A simple demonstration of Eq. (A3) can be found in the last part of the appendix.

The sum of all the helicity amplitudes of the subprocess $g + g \rightarrow (cc) + \bar{c} + \bar{c}$ can be arranged as

$$M^{(\lambda_2, \lambda_4, \lambda_5, \lambda_6)}(q_{c3}, q_{c4}, q_{c1}, q_{c2}, k_1, k_2) = \sum_{m=1}^6 C_{mij} M_m^{(\lambda_2, \lambda_4, \lambda_5, \lambda_6)}(q_{c3}, q_{c4}, q_{c1}, q_{c2}, k_1, k_2), \quad (\text{A4})$$

where C_{mij} ($m = 1-6$) are six independent color factors of the process,

$$\begin{aligned} C_{1ij} &= \frac{1}{2\sqrt{2}} (T^a T^b)_{mi} G_{mjk}, \\ C_{2ij} &= \frac{1}{2\sqrt{2}} (T^b T^a)_{mi} G_{mjk}, \\ C_{3ij} &= \frac{1}{2\sqrt{2}} (T^a)_{mj} (T^b)_{ni} G_{mnk}, \\ C_{4ij} &= \frac{1}{2\sqrt{2}} (T^b)_{mj} (T^a)_{ni} G_{mnk}, \\ C_{5ij} &= \frac{1}{2\sqrt{2}} (T^a T^b)_{mj} G_{mik}, \\ C_{6ij} &= \frac{1}{2\sqrt{2}} (T^b T^a)_{mj} G_{mik}, \end{aligned} \quad (\text{A5})$$

where $i, j = 1, 2, 3$ are color indices of the two outgoing antiquarks \bar{c} and \bar{c} respectively, and the indices a and b are color indices for gluon-1 and gluon-2, respectively. Here, the function G_{mjk} equals to the antisymmetric ε_{mjk} for the (cc) -diquark in $\mathbf{\bar{3}}$ configuration and equals to the symmetric f_{mjk} for the (cc) -diquark in $\mathbf{6}$ configuration, respectively. The antisymmetric ε_{mjk} satisfies $\varepsilon_{mjk} \varepsilon_{m'j'k} = \delta_{mm'} \delta_{jj'} - \delta_{mj'} \delta_{jm'}$ and the symmetric f_{mjk} satisfies $f_{mjk} f_{m'j'k} = \delta_{mm'} \delta_{jj'} + \delta_{mj'} \delta_{jm'}$.

TABLE V. The square of the six independent color factors (including the cross terms) for $gg \rightarrow (cc)_3[{}^3S_1] + \bar{c} + \bar{c}$, ($C_{mij} \times C_{nij}^*$) with $m, n = (1, 2, \dots, 6)$, respectively.

	C_{1ij}^*	C_{2ij}^*	C_{3ij}^*	C_{4ij}^*	C_{5ij}^*	C_{6ij}^*
C_{1ij}	$\frac{4}{3}$	$-\frac{1}{6}$	$\frac{2}{3}$	$-\frac{1}{12}$	$\frac{5}{12}$	$-\frac{1}{3}$
C_{2ij}	$-\frac{1}{6}$	$\frac{4}{3}$	$-\frac{1}{12}$	$\frac{2}{3}$	$-\frac{1}{3}$	$\frac{5}{12}$
C_{3ij}	$\frac{2}{3}$	$-\frac{1}{12}$	$\frac{4}{3}$	$-\frac{5}{12}$	$\frac{1}{12}$	$-\frac{2}{3}$
C_{4ij}	$-\frac{1}{12}$	$\frac{2}{3}$	$-\frac{5}{12}$	$\frac{4}{3}$	$-\frac{2}{3}$	$\frac{1}{12}$
C_{5ij}	$\frac{5}{12}$	$-\frac{1}{3}$	$\frac{1}{12}$	$-\frac{2}{3}$	$\frac{4}{3}$	$-\frac{1}{6}$
C_{6ij}	$-\frac{1}{3}$	$\frac{5}{12}$	$-\frac{2}{3}$	$\frac{1}{12}$	$-\frac{1}{6}$	$\frac{4}{3}$

TABLE VI. The square of the six independent color factors (including the cross terms) for $gg \rightarrow (cc)_6[{}^1S_0] + \bar{c} + \bar{c}$, ($C_{mij} \times C_{nij}^*$) with $m, n = (1, 2, \dots, 6)$, respectively.

	C_{1ij}^*	C_{2ij}^*	C_{3ij}^*	C_{4ij}^*	C_{5ij}^*	C_{6ij}^*
C_{1ij}	$\frac{8}{3}$	$-\frac{1}{3}$	$\frac{2}{3}$	$-\frac{1}{12}$	$\frac{11}{12}$	$\frac{1}{6}$
C_{2ij}	$-\frac{1}{3}$	$\frac{8}{3}$	$-\frac{1}{12}$	$\frac{2}{3}$	$\frac{1}{6}$	$\frac{11}{12}$
C_{3ij}	$\frac{2}{3}$	$-\frac{1}{12}$	$\frac{8}{3}$	$\frac{11}{12}$	$-\frac{1}{12}$	$\frac{2}{3}$
C_{4ij}	$-\frac{1}{12}$	$\frac{2}{3}$	$\frac{11}{12}$	$\frac{8}{3}$	$\frac{2}{3}$	$-\frac{1}{12}$
C_{5ij}	$\frac{11}{12}$	$\frac{1}{6}$	$-\frac{1}{12}$	$\frac{2}{3}$	$\frac{8}{3}$	$-\frac{1}{3}$
C_{6ij}	$\frac{1}{6}$	$\frac{11}{12}$	$\frac{2}{3}$	$-\frac{1}{12}$	$-\frac{1}{3}$	$\frac{8}{3}$

To get the matrix element squared, one needs to deal with the square of the above six independent color factors as shown in Eq. (A5) (including the cross terms), i.e. ($C_{mij} \times C_{nij}^*$) with $m, n = (1, 2, \dots, 6)$. For reference use, we list the square of these six independent color factors in Table V and VI, which are for $(cc)_3[{}^3S_1]$ and $(cc)_6[{}^1S_0]$, respectively.

By keeping all these points in mind, we rewrite a program based on the B_c meson generator BCVEGPY [19,20] to calculate the gluon-gluon fusion mechanism for the hadronic production of Ξ_{cc} .

Finally, we give a simple demonstration of the relation Eq. (A3). To demonstrate the relation Eq. (A3), we shall adopt the following relation,

$$\langle p_{(\lambda_1)} | \not{k}_1 \dots \not{k}_n | q_{(\lambda_2)} \rangle = (-1)^{n+1} \langle q_{(-\lambda_2)} | \not{k}_n \dots \not{k}_1 | p_{(-\lambda_1)} \rangle, \quad (\text{A6})$$

whose nonzero ones can be explicitly written as [30]

$$\langle p_- | \not{k}_1 \dots \not{k}_n | q_+ \rangle = -\langle q_- | \not{k}_n \dots \not{k}_1 | p_+ \rangle (n \text{ even}), \quad (\text{A7})$$

$$\langle p_+ | \not{k}_1 \dots \not{k}_n | q_- \rangle = -\langle q_+ | \not{k}_n \dots \not{k}_1 | p_- \rangle (n \text{ even}), \quad (\text{A8})$$

$$\langle p_+ | \not{k}_1 \dots \not{k}_n | q_+ \rangle = \langle q_- | \not{k}_n \dots \not{k}_1 | p_- \rangle (n \text{ odd}), \quad (\text{A9})$$

where k_i ($i = 1, \dots, n$) are any types of momenta.

Generally, to the i -th Feynman diagram, we can expand Γ_i as,

$$\Gamma_i = \sum_n C_n (\not{p}_1 \not{p}_2 \dots \not{p}_n), \quad (\text{A10})$$

and then we have,

$$\hat{\Gamma}_i = \sum_n (-1)^n C_n (\not{p}_n \dots \not{p}_2 \not{p}_1), \quad (\text{A11})$$

where C_n are functions free of Dirac γ matrix element. Taking use of Eq. (A6), we finally obtain

$$\begin{aligned}
\langle q_{0(-\lambda_1)} | (\not{d}_{c3} + m_c) \Gamma_{2i} (\not{d}_{c4} - m_c) | q_{0(-\lambda_2)} \rangle &= \sum_n C_n \langle q_{0(-\lambda_1)} | [\not{d}_{c3} (\not{p}_1 \not{p}_2 \cdots \not{p}_n) \not{d}_{c4} - m_c \not{d}_{c3} (\not{p}_1 \not{p}_2 \cdots \not{p}_n) \\
&\quad + m_c (\not{p}_1 \not{p}_2 \cdots \not{p}_n) \not{d}_{c4} - m_c^2 (\not{p}_1 \not{p}_2 \cdots \not{p}_n)] | q_{0(-\lambda_2)} \rangle \\
&= \sum_n C_n \langle q_{0(\lambda_2)} | [(-1)^{n+3} \not{d}_{c4} (\not{p}_n \cdots \not{p}_2 \not{p}_1) \not{d}_{c3} - (-1)^{n+2} m_c (\not{p}_n \cdots \not{p}_2 \not{p}_1) \not{d}_{c3} \\
&\quad + (-1)^{n+2} m_c \not{d}_{c4} (\not{p}_n \cdots \not{p}_2 \not{p}_1) - (-1)^{n+1} m_c^2 (\not{p}_n \cdots \not{p}_2 \not{p}_1)] | q_{0(\lambda_1)} \rangle \\
&= -\langle q_{0(\lambda_2)} | (\not{d}_{c4} + m_c) \hat{\Gamma}_{2i} (\not{d}_{c3} - m_c) | q_{0(\lambda_1)} \rangle. \tag{A12}
\end{aligned}$$

APPENDIX B: CALCULATION TECHNOLOGY IN FDC PROGRAM AND THE SQUARE OF AMPLITUDE FOR THE EXTRINSIC CHARM MECHANISM

First, we take gluon-gluon fusion mechanism as an explicit example to show the technology in FDC program [21] and show in detail how we can derive the program for the hadronic production of Ξ_{cc} from those of J/ψ .

The amplitude for each Feynman diagram of $g + g \rightarrow J/\psi(p_3) + c(p_4) + \bar{c}(p_5)$ can be written as:

$$\begin{aligned}
M(J/\psi) &= \bar{u}(p_4, s_4) \Gamma_1 s_f(k_1, m_c) \cdots s_f(k_{n-1}, m_c) \Gamma_n v\left(\frac{p_3}{2}, s_1\right) \\
&\quad \times B(p_3, s, s_1, s_2, m_{J/\psi}) \bar{u}\left(\frac{p_3}{2}, s_2\right) \\
&\quad \times \Gamma'_1 s_f(q_1, m_c) \cdots s_f(q_{n'-1}, m_c) \Gamma'_{n'} v(p_5, s_5). \tag{B1}
\end{aligned}$$

where $s_f(k, m)$ ($k = k_i$ or q_i) is the fermion propagator, $B(p_3, s, s_1, s_2, m_{J/\psi})$ is the wave function of J/ψ , $\Gamma_1, \cdots, \Gamma_n, \Gamma'_1, \cdots, \Gamma'_{n'}$, are the interaction vertices. The color factor part is treated separately (similar to the method described in Appendix. A) and will not discussed here.

One can easily find out the corresponding Feynman diagram in $g + g \rightarrow \Xi_{cc}(p_3) + \bar{c}(p_4) + \bar{c}(p_5)$ and the amplitude of it could be written as:

$$\begin{aligned}
M(\Xi_{cc}) &= \bar{u}\left(\frac{p_3}{2}, s_1\right) \Gamma_n s_f(-k_{n-1}, m_c) \cdots s_f(-k_1, m_c) \\
&\quad \times \Gamma_1 v(p_4, s_4) B(p_3, s, s_1, s_2, m_{\Xi_{cc}}) \bar{u}\left(\frac{p_3}{2}, s_2\right) \\
&\quad \times \Gamma'_1 s_f(q_1, m_c) \cdots s_f(q_{n'-1}, m_c) \Gamma'_{n'} v(p_5, s_5), \tag{B2}
\end{aligned}$$

where $B(p_3, s, s_1, s_2, m_{\Xi_{cc}})$ is the wave function of Ξ_{cc} . For an arbitrary Fermion line,

$$a = \bar{u}\left(\frac{p_3}{2}, s_1\right) \Gamma_n s_f(-k_{n-1}, m_c) \cdots s_f(-k_1, m_c) \Gamma_1 v(p_4, s_4),$$

we have

$$a = a^T$$

$$\begin{aligned}
&= v^T(p_4, s_4) \Gamma_1^T s_f^T(-k_1, m_c) \cdots s_f^T(-k_{n-1}, m_c) \Gamma_n^T \bar{u}\left(\frac{p_3}{2}, s_1\right)^T \\
&= v^T(p_4, s_4) C C^- \Gamma_1^T C C^- s_f^T(-k_1, m_c) C C^- \cdots \\
&\quad \times C C^- s_f^T(-k_{n-1}, m_c) C C^- \Gamma_n^T C C^- \bar{u}\left(\frac{p_3}{2}, s_1\right)^T \\
&= (-1)^{(n+1)} \bar{u}(p_4, s_4) \Gamma_1 s_f(k_1, m_c) \cdots s_f(k_{n-1}, m_c) \\
&\quad \times \Gamma_n v\left(\frac{p_3}{2}, s_1\right),
\end{aligned}$$

with the help of the following equations

$$\begin{aligned}
v^T(p_4, s_4) C &= -\bar{u}(p_4, s_4), \quad C^- \bar{u}\left(\frac{p_3}{2}, s_1\right)^T = v\left(\frac{p_3}{2}, s_1\right), \\
C^- \Gamma_i^T C &= -\Gamma_i, \quad C^- s_f^T(-k_i, m_c) C = s_f(k_i, m_c).
\end{aligned}$$

Where $C = -i\gamma^2\gamma^0$ is the charge conjugation matrix. And then Eq. (B2) can be transformed as

$$\begin{aligned}
M(\Xi_{cc}) &= (-1)^{(n+1)} \bar{u}(p_4, s_4) \Gamma_1 s_f(k_1, m_c) \cdots s_f(k_{n-1}, m_c) \\
&\quad \times \Gamma_n v\left(\frac{p_3}{2}, s_1\right) B(p_3, s, s_1, s_2, m_{\Xi_{cc}}) \bar{u}\left(\frac{p_3}{2}, s_2\right) \\
&\quad \times \Gamma'_1 s_f(q_1, m_c) \cdots s_f(q_{n'-1}, m_c) \Gamma'_{n'} v(p_5, s_5). \tag{B3}
\end{aligned}$$

By comparing Eq. (B1) with Eq. (B3), one find that they are the same except for an overall factor $(-1)^{(n+1)}$, where ‘ n ’ is the interaction vertex number of the corresponding fermion line and depends on the detail of each Feynman diagram. Therefore, we can completely use the method of J/ψ to deal with Ξ_{cc} case by adding a factor $(-1)^{(n+1)}$ diagram by diagram. The detailed description of method to treat the J/ψ and B_c calculation could be found in the Ref. [20,21].

All the above discussion is also valid for the calculation of the ‘‘extrinsic’’ charm mechanisms. And the following results are obtained by taking the FDC program.

For convenience, we express the square of the amplitudes by the variants s, t and u , which are defined as:

$$\begin{aligned}
s &= (p_1 + p_2)^2, \quad t = (p_1 - p_3)^2, \\
u &= (p_1 - p_4)^2,
\end{aligned}$$

where $p_i = (E_i, p_{ix}, p_{iy}, p_{iz})$ are the corresponding momenta for the involved particles: p_1 and p_2 are the momenta of initial partons, p_3 and p_4 are the momenta of Ξ_{cc} and another outgoing particles, respectively. Further more, for $\bar{c}(p_1) + g(p_2) \rightarrow \Xi_{cc}(p_3) + \bar{c}(p_4)$, we set

$$u_1 = (u - 4m_c^2), \quad s_1 = (s - m_c^2), \quad t_1 = (t - m_c^2),$$

and for $c(p_1) + c(p_2) \rightarrow \Xi_{cc}(p_3) + g(p_4)$, we set

$$u_1 = (u - m_c^2), \quad s_1 = (s - 4m_c^2), \quad t_1 = (t - m_c^2).$$

The relation, $u_1 + t_1 + s_1 = 0$, is useful to make all the expressions for the square of the amplitudes compact.

The square of the amplitude for the subprocess $c(p_1) + g(p_2) \rightarrow \Xi_{cc}(p_3) + \bar{c}(p_4)$ with (cc) -diquark in $(cc)_3[{}^3S_1]$ can be written as,

$$|\bar{M}|^2 = \frac{2^9 \alpha_s^3 |\Psi_{cc}(0)|^2 \pi^4}{3^5 M} \left[4M^2 \left(\frac{10}{u_1^2} + \frac{-4}{s_1 t_1} + \frac{11u_1^2}{s_1^2 t_1^2} + \frac{4u_1^4}{s_1^3 t_1^3} \right) + 4M^4 \left(\frac{-17}{s_1 t_1 u_1} + \frac{28u_1}{s_1^2 t_1^2} + \frac{-20u_1^3}{s_1^3 t_1^3} \right) + 3M^6 \left(\frac{-12}{s_1 t_1 u_1^2} + \frac{-5}{s_1^2 t_1^2} + \frac{-14u_1^2}{s_1^3 t_1^3} + \frac{4u_1^4}{s_1^4 t_1^4} \right) + 8 \left(\frac{-2}{u_1} + \frac{11u_1}{s_1 t_1} + \frac{-9u_1^3}{s_1^2 t_1^2} \right) \right]. \quad (\text{B4})$$

The square of the amplitude for the subprocess $c(p_1) + g(p_2) \rightarrow \Xi_{cc}(p_3) + \bar{c}(p_4)$ with (cc) -diquark in $(cc)_6[{}^1S_0]$ can be written as,

$$|\bar{M}|^2 = \frac{2^9 \alpha_s^3 |\Psi_{cc}(0)|^2 \pi^4}{3^5 M} \left[M^2 \left(\frac{-20}{u_1^2} + \frac{-1}{s_1 t_1} + \frac{-12u_1^2}{s_1^2 t_1^2} \right) + 4M^4 \left(\frac{-12}{s_1 t_1 u_1} + \frac{-u_1}{s_1^2 t_1^2} + \frac{-2u_1^3}{s_1^3 t_1^3} \right) + M^6 \left(\frac{-48}{s_1 t_1 u_1^2} + \frac{8}{s_1^2 t_1^2} + \frac{-7u_1^2}{s_1^3 t_1^3} + \frac{2u_1^4}{s_1^4 t_1^4} \right) + 2 \left(\frac{-10}{u_1} + \frac{9u_1}{s_1 t_1} + \frac{-2u_1^3}{s_1^2 t_1^2} \right) \right]. \quad (\text{B5})$$

The square of the amplitude for the subprocess $c(p_1) + c(p_2) \rightarrow \Xi_{cc}(p_3) + g(p_4)$ with (cc) -diquark in $(cc)_3[{}^3S_1]$ can be written as,

$$|\bar{M}|^2 = \frac{2^{11} \alpha_s^3 |\Psi_{cc}(0)|^2 \pi^4}{3^6 M} \left[4M^2 \left(\frac{-4s_1^4}{t_1^3 u_1^3} + \frac{11s_1^3}{t_1^2 u_1^3} + \frac{15s_1^2}{t_1 u_1^3} + \frac{18s_1}{u_1^3} + \frac{34t_1}{u_1^3} + \frac{30t_1^2}{s_1 u_1^3} + \frac{10t_1^3}{s_1 u_1^3} \right) + 4M^4 \left(\frac{20s_1^3}{t_1^3 u_1^3} + \frac{28s_1^2}{t_1^2 u_1^3} + \frac{28s_1}{t_1 u_1^3} + \frac{17}{s_1 t_1 u_1} \right) + 3M^6 \left(\frac{-4s_1^4}{t_1^4 u_1^4} + \frac{-14s_1^3}{t_1^3 u_1^4} + \frac{-9s_1^2}{t_1^2 u_1^4} + \frac{-2s_1}{t_1 u_1^4} + \frac{-31}{u_1^4} + \frac{-36t_1}{s_1 u_1^4} + \frac{-12t_1^2}{s_1^2 u_1^4} \right) + 8 \left(\frac{9s_1^3}{t_1^2 u_1^2} + \frac{11s_1^2}{t_1 u_1^2} + \frac{11s_1}{u_1^2} + \frac{2}{s_1} \right) \right]. \quad (\text{B6})$$

The square of the amplitude for the subprocess $c(p_1) + c(p_2) \rightarrow \Xi_{cc}(p_3) + g(p_4)$ with (cc) -diquark in $(cc)_6[{}^1S_0]$ can be written as,

$$|\bar{M}|^2 = \frac{2^{11} \alpha_s^3 |\Psi_{cc}(0)|^2 \pi^4}{3^6 M} \left[M^2 \left(\frac{12s_1^2}{t_1^2 u_1^2} + \frac{-s_1}{t_1 u_1^2} + \frac{-1}{u_1^2} + \frac{20}{s_1^2} \right) + 4M^4 \left(\frac{2s_1^3}{t_1^3 u_1^3} + \frac{-s_1^2}{t_1^2 u_1^3} + \frac{-s_1}{t_1 u_1^3} + \frac{12}{s_1 t_1 u_1} \right) + M^6 \left(\frac{-2s_1^4}{t_1^4 u_1^4} + \frac{-7s_1^3}{t_1^3 u_1^4} + \frac{-15s_1^2}{t_1^2 u_1^4} + \frac{-64s_1}{t_1 u_1^4} + \frac{-152}{u_1^4} + \frac{-144t_1}{s_1 u_1^4} + \frac{-48t_1^2}{s_1^2 u_1^4} \right) + 2 \left(\frac{2s_1^3}{t_1^2 u_1^2} + \frac{9s_1^2}{t_1 u_1^2} + \frac{9s_1}{u_1^2} + \frac{10}{s_1} \right) \right]. \quad (\text{B7})$$

In these equation, M is the mass of Ξ_{cc} and $\Psi_{cc}(0)$ is the wave function at origin for the $[{}^3S_1] cc$ state. And here we have adopted that $h_3 = |\Psi_{cc}(0)|^2$ and $h_1 = h_3$.

- [1] M. Mattson *et al.* (SELEX Collaboration), Phys. Rev. Lett. **89**, 112001 (2002).
 [2] A. Ocherashvili *et al.* (SELEX Collaboration), Phys. Lett.

- B 628**, 18 (2005).
 [3] V. V. Kiselev and A. K. Likhoded, hep-ph/0208231.
 [4] M. Moinester, Z. Phys. A **355**, 349 (1996); V. V. Kiselev

- and A. Likhoded, Phys. Usp. **45**, 455 (2002).
- [5] S. P. Baranov, Phys. Rev. D **54**, 3228 (1996).
- [6] A. V. Berezhnoy, V. V. Kiselev, A. K. Likhoded, and A. I. Onishchenko, Phys. Rev. D **57**, 4385 (1998).
- [7] A. V. Berezhnoy, V. V. Kiselev, and A. K. Likhoded, Phys. At. Nucl. **59**, 870 (1996).
- [8] A. V. Berezhnoy, V. V. Kiselev, and A. K. Likhoded, Sov. J. Nucl. Phys. **59**, 909 (1996).
- [9] J. P. Ma and Z. G. Si, Phys. Lett. B **568**, 135 (2003).
- [10] G. T. Bodwin, E. Braaten, and G. P. Lepage, Phys. Rev. D **51**, 1125 (1995); **55**, 5853(E) (1997).
- [11] Cong-Feng Qiao, J. Phys. G **29**, 1075 (2003); hep-ph/0202227.
- [12] Chao-Hsi Chang, Cong-Feng Qiao, Jian-Xiong Wang, and Xing-Gang Wu, Phys. Rev. D **72**, 114009 (2005).
- [13] S. Kretzer, H. L. Lai, F. I. Olness, and W. K. Tung, Phys. Rev. D **69**, 114005 (2004).
- [14] R. Vogt and S. J. Brodsky, Nucl. Phys. **B478**, 311 (1996).
- [15] F. I. Olness, R. J. Scalise, and W. T. Tung, Phys. Rev. D **59**, 014506 (1999).
- [16] M. A. G. Aivazis, J. C. Collins, F. I. Olness, and W. K. Tung, Phys. Rev. D **50**, 3102 (1994); Phys. Rev. D **50**, 3085 (1994).
- [17] J. Amundson, C. Schmidt, W. K. Tung, and X. N. Wang, J. High Energy Phys. **10** (2000) 031.
- [18] D. A. Günter and V. A. Saleev, Phys. Rev. D **64**, 034006 (2001).
- [19] Chao-Hsi Chang, Chafik Driouich, Paula Eerola, and Xing-Gang Wu, Comput. Phys. Commun. **159**, 192 (2004).
- [20] Chao-Hsi Chang, Jian-Xiong Wang, and Xing-Gang Wu, Comput. Phys. Commun. **174**, 241 (2006).
- [21] Jian-Xiong Wang, Nucl. Instrum. Methods Phys. Res., Sect. A **534**, 241 (2004).
- [22] R. Kleiss and W. J. Stirling, Comput. Phys. Commun. **40**, 359 (1986).
- [23] G. P. Lepage, J. Comput. Phys. **27**, 192 (1978).
- [24] Chao-Hsi Chang, Shao-Long Chen, Tai-Fu Feng, and Xue-Qian Li, Phys. Rev. D **64**, 014003 (2001).
- [25] J. Pumplin, D. R. Stump, J. Huston, H. L. Lai, P. Nadolsky, and W. K. Tung, J. High Energy Phys. **07** (2002) 012.
- [26] M. Klasen, B. A. Kniehl, L. N. Mihaila, and M. Steihauser, Phys. Rev. Lett. **89**, 032001 (2002); Chao-Hsi Chang and Xing-Gang Wu, Eur. Phys. J. C **38**, 267 (2004); Chao-Hsi Chang, Jian-Xiong Wang, and Xing-Gang Wu, Phys. Rev. D **70**, 114019 (2004); N. Brambilla *et al.*, hep-ph/0412158.
- [27] Chao-Hsi Chang *et al.* (unpublished).
- [28] Jon Pumplin, hep-ph/0508184.
- [29] S. J. Brodsky, P. Hoyer, C. Peterson, and N. Sakai, Phys. Lett. B **93**, 451 (1980); S. J. Brodsky, C. Peterson, and N. Sakai, Phys. Rev. D **23**, 2745 (1981); T. Gutierrez and R. Vogt, Nucl. Phys. **B539**, 189 (1999); G. Ingelman and M. Thunman, Z. Phys. C **73**, 505 (1997).
- [30] Zhan Xu, Da-Hua Zhang, and Lee Chang, Nucl. Phys. **B291**, 392 (1987).